

INVESTIGATION OF Cr DOPED CdTe FOR OPTOELECTRONIC AND SPINTRONIC DEVICES APPLICATIONS

M. YASEEN^a, H. AMBREEN^a, U. SHOUKAT^a, M. K. BUTT^a, S. NOREEN^b,
S. U. REHMAN^b, J. IQBAL^b, S. BIBI^b, A. MURTAZA^c, S. M. RAMAY^{d*}

^aDepartment of Physics, University of Agriculture, Faisalabad 38040, Pakistan

^bDepartment of Chemistry, University of Agriculture, Faisalabad 38040, Pakistan

^cSchool of Science, MOE Key Laboratory for Nonequilibrium Synthesis and Modulation of Condensed Matter, State Key Laboratory for Mechanical Behaviour of Materials, Xi'an Jiaotong University, Xi'an 710049, China

^dPhysics and Astronomy Department, College of Science, King Saud University, Riyadh, Saudi Arabia

Electronic, optical and magnetic properties of Cr doped CdTe dilute magnetic semiconductors were studied by using density functional theory (DFT). Electronic band structure and density of states (DOS) for spin-up and spin-down states were investigated which confirmed the half metallic ferromagnetic (HMF) behavior of synthesized material. Band gap increased from 0.73 to 1.41 eV in spin-downstate by Cr doping of 6.25% to 25% in CdTe binary compound. In optical properties, optical conductivity, absorption coefficient, extinction coefficient, real and imaginary parts of dielectric function and refractive index were studied in detail. It was observed that Cr play important role in the ferromagnetic behavior of $Cd_{1-x}Cr_xTe$ compound. Results revealed that $Cd_{1-x}Cr_xTe$ is a promising candidate for optoelectronics and spintronics devices applications.

(Received August 9, 2019; Accepted December 2, 2019)

Keywords: Optical properties, Band structure, Spintronics, Density of states

1. Introduction

During the last few years, half metallic ferromagnetic (HMF) materials have been studied widely due to their applications in spintronics and optoelectronics devices. Half metallic ferromagnetic materials consist of two spin version, one spin version act as a semiconductor or insulator with considerable energy gap around the fermi level while other act as metallic [1]. Some of the materials have been described as a spin gapless semiconductor, in which one spin channel has almost zero width energy gap around fermi level while the other spin channel has energy gap [2]. In 1983, Groot *et al.*, gives the concept of half metallic ferromagnetic material by using the band structures of the half-Heusler compound such as NiMnSb[3]. For the predication of half metallic ferromagnetic behavior, different materials such as Co_2FeSi [4], Fe_3O_4 [5], full-Heusler compounds such as Co_2MnSi [6], CrO_2 [7], perovskite alloys such as Sr_2FeMoO_6 [8] and $La_{0.7}Sr_{0.3}MnO_3$ [9] have been studied theoretically and confirmed by experimentally [10].

Investigation of transition metals in binary compounds is beneficial to make the new devices of spintronics such as light emitted diodes, logic devices, spin valves, ultra-fast optical switches and magnetic sensors [11-12]. A lot of efforts have been made to investigate the mechanism behind HMF and other physical properties, in order to discover the new half-metallic ferromagnetic materials which are more auspicious for applications and basic properties are still very important [13]. Diluted magnetic semiconductors (DMSs) have also been used to originate the half metallic ferromagnetic properties [14-16].

In this work, electronic, magnetic and optical properties of Cr doped CdTe are systematically studied in detail. Transition metal (Cr) was used as a doping element in CdTe compound to investigate the spin polarization.

*Corresponding author: schaudhry@ksu.edu.sa

2. Method of calculation

Full potential linearized augmented plane wave method (FP-LMTO) [17] with density functional theory [18] was used to calculate the properties of materials [18-19] by using Wein2k code [19]. PBE-GGA was used to measure exchange correlation potential [20-21]. The core state electrons are used for the solution of Dirac equation by ignoring the spin-orbit coupling [22]. The maximum value of angular momentum was taken $l_{\max}=10$. To check the energy eigenvalue convergence 35 **k**-points meshes were used for binary compound which expand the wave function up to $K_{\max} R_{\text{MT}}=8$ where R_{MT} represent the muffin-tin atomic radius and K_{\max} represent the maximum value of reciprocal vector which are used to get the total energy convergence which was less than the 0.00001 Ryd [23]. The states of Te ($4d^{10} 5s^2 5p^4$) and Cd ($4d^{10} 5s^2$) are behaved as valance electrons. The muffin-tin radii for Te and Cd were 2.4 and 2.3 a.u, respectively [24].

3. Results and discussions

3.1. Electronic Properties

Electronic bands structure of Cr doped CdTe compound at $X = 6.25\%$, 12.50% and 25% are illustrated in Fig. 1. In the band structures the conducting nature have been observed in spin-up channel due to the overlapping of conduction and valance bands, and the semiconductor nature have been observed in spin-dn version because some of the conduction band (CB) states are located in valance band (VB) states resulting the large energy bandgap (E_g) around the Fermi level.

In Fig.1, the maxima of valance bands and minima of conduction bands are located at the Γ point of first Brillouin-zone and shows direct band gap. Cr doped CdTe compound gives different energy band plots.

The calculated band gap for pure CdTe is 0.4 eV but after the doping of the transition metal in CdTe compound the band gap first increased and later decreased. At the concentration of 6.25% & 12.50% the band gap was 0.73 and 1.41 eV, respectively, but after the 25% doping the band gap again decreased to 1.03 eV. The doping of Cr causes the increase in energy gap for spin-up channel and decrease in energy gap for spin-dn channel. The calculated band structures for $\text{Cd}_{1-x}\text{Cr}_x\text{Te}$ ($X = 6.25\%$, 12.5% and 25%) shows a half metallic ferromagnetic nature. The nature of electronic band structures is also studied by the total density of states (TDOS) and the partial density of states (PDOS) of pure CdTe and $\text{Cd}_{1-x}\text{Cr}_x\text{Te}$.

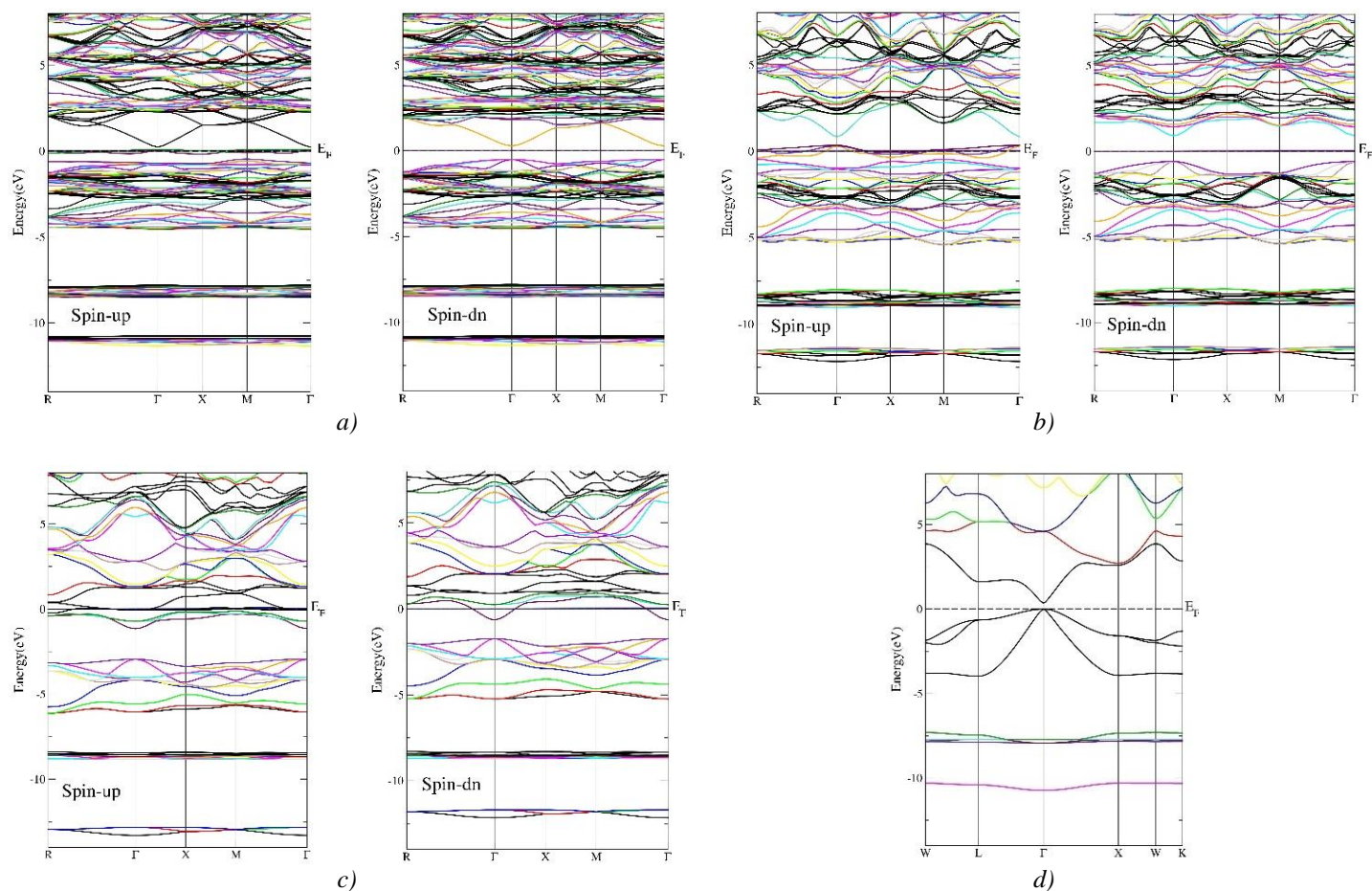


Fig. 1. Spin-Polarized energy band plot of $Cd_{1-x}Cr_xTe$ (a) $x = 6.25\%$, (b) $x = 12.5\%$, (c) $x = 25\%$, (d) Pure CdTe compound.

Partial and total density of states curves are shown in Fig. 2 (a, b & c). Graphs shows that Cr doped CdTe compound exhibits a half metallic ferromagnetic behavior as the density of states (DOS) passes fermi level in the spin up version, and it is also clear from figure that the peaks around the fermi level is mainly contributed by the $3d$ states of Cr. Total density of states at 6.25% showed the energy gap about 0.73 in the spin-dn channel, and the contribution of Cd- d and Cr- d is large as compare to all other orbits in partial density of states (POS).The energy gap is obtained due to the hybridization of the $3d$ -state of transition metal, d , p -state of Cd and p state of Te as shown in Fig. 2 (c). The TDOS at 12.5% concentration of Cr shows energy gap about 1.41 in the spin-dn channel and showed overlapping in spin-up channel. The main contribution in PDOS is due to $3d$ orbit of Cr and d orbit of Cd but the contribution of Te- p is small as compare to the Cd and Cr.The energy gap is due to the hybridization of the d and p orbital of Cd and p orbital of Te mainly contribute to the states near the fermi region as shown in Fig.2 (d, e&f). At 25% concentration of Cr in CdTe compound the band gap was about 1.03 in spin-dn version as shown in Fig.2 (g, h & k). The diversity of band gaps indicates applications of the compound in the spintronic devices such as memory storage.

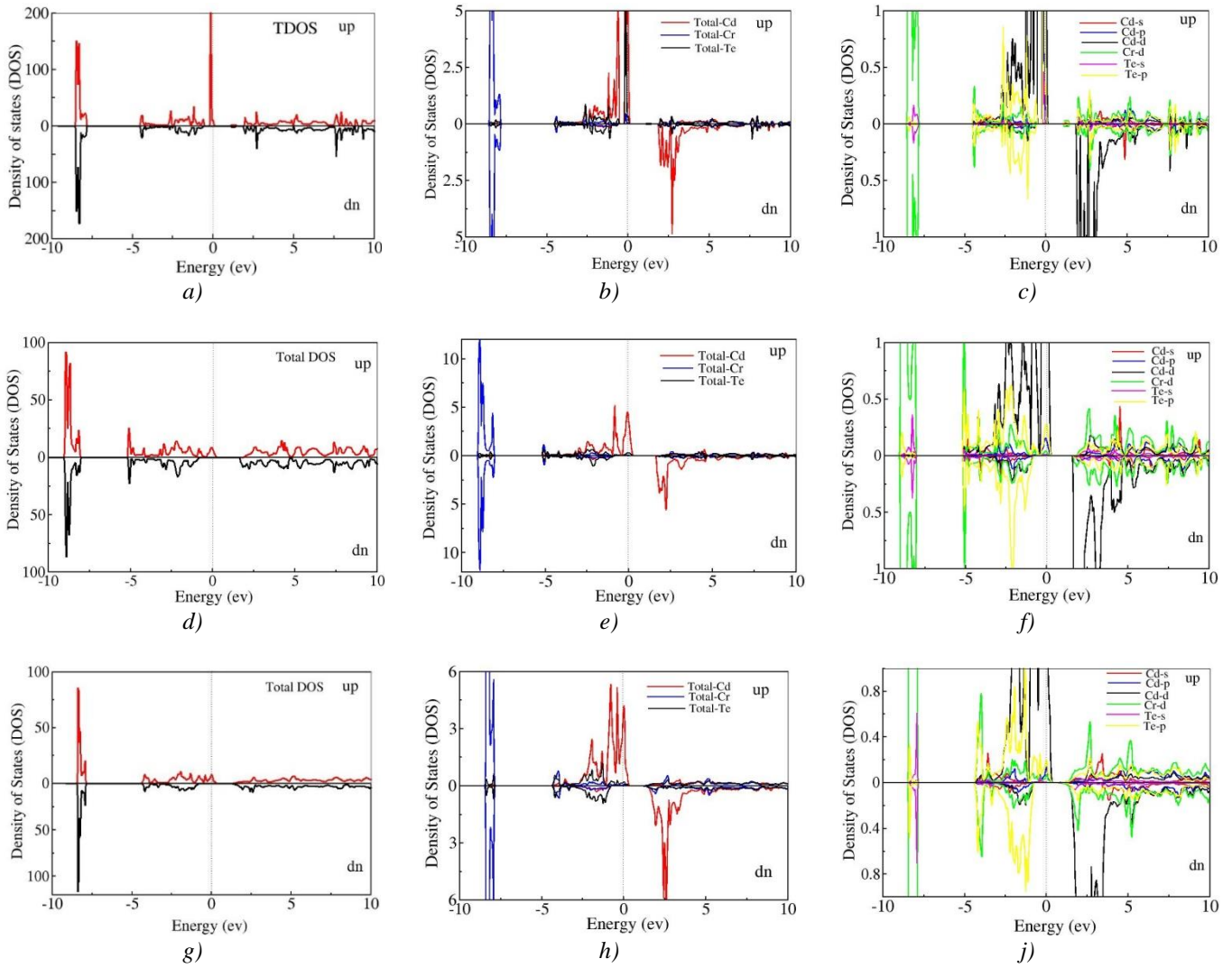


Fig. 2. (a & b). Spin-Polarized total density of states of $\text{Cd}_{1-x}\text{Cr}_x\text{Te}$ (c) partial density of states at $x = 6.25\%$, (d & e) total density of states and partial density of states at $x = 12.5\%$, (g & h) total density of states and partial density of states at $x = 25\%$.

3.2. Optical properties

Optical transitions occur between unoccupied and occupied states due to the electric field of photon, so the optical properties of the medium can be derived from the complex dielectric function $\epsilon(\omega) = \epsilon_1(\omega) + i\epsilon_2(\omega)$.

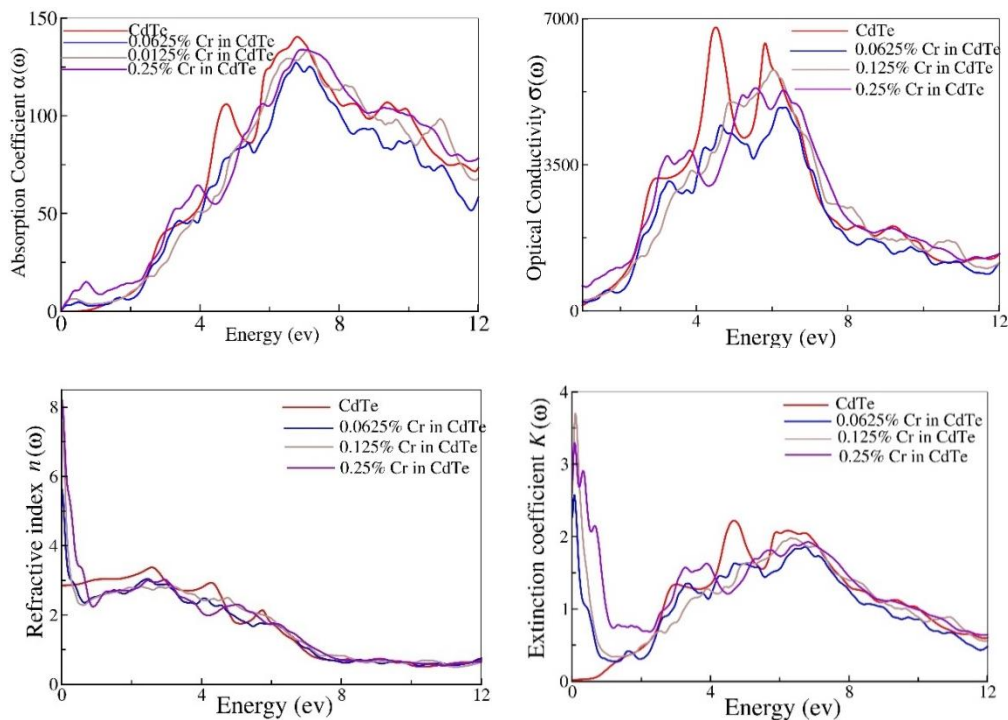


Fig. 3. (a) Absorption coefficient (b) optically conductivity (c) refractive index of pure (d) extinction coefficient of Pure CdTe and $Cd_{1-x}Cr_xTe$ ($x = 6.25\%$, 12.5% , 25%).

Kramers–Kronig transformation are used to calculate the real part of dielectric function $\epsilon_1(\omega)$ while the imaginary part of the dielectric function $\epsilon_2(\omega)$ are calculated by many-electron wavefunction [25]. The peaks in the imaginary part of dielectric function are directly connected to various intra-band and inter-band transitions in the first irreducible Brillion zone. All other optical constants such as optical conductivity $I(\omega)$, absorption coefficient $\sigma(\omega)$, refractive index $n(\omega)$, reflectivity $R(\omega)$, extinction coefficient $k(\omega)$ are basically attained from imaginary part $\epsilon_2(\omega)$ and real part $\epsilon_1(\omega)$ of dielectric function [26-28].

By the following formulas:

$$I(\omega) = \frac{4\pi}{\lambda} \left(\frac{[\epsilon_1^2(\omega) + \epsilon_2^2(\omega)]^{1/2} + \epsilon_1(\omega)}{2} \right)^{1/2} \quad (1)$$

$$\sigma(\omega) = \frac{\omega}{4\pi} \epsilon_2(\omega) \quad (2)$$

$$n(\omega) = \left(\frac{[\epsilon_1^2(\omega) + \epsilon_2^2(\omega)]^{1/2} + \epsilon_1(\omega)}{2} \right)^{1/2} \quad (3)$$

$$k(\omega) = \frac{\alpha\lambda}{4\pi} \quad (4)$$

$$R(\omega) = \frac{[n(\omega)-1]^2 + k^2(\omega)}{[n(\omega)+1]^2 + k^2(\omega)} \quad (5)$$

$$\epsilon_2(\omega) = \frac{Ve^2}{2\pi\hbar m^2 \omega^2} \int d^3k \sum_{nn'} l \langle kn|p|kn' \rangle l^2 f(kn) \times (1 - f(kn')) \delta(E_{kn} - E_{kn'} - \hbar\omega) \quad (6)$$

where λ , ω , ϵ_1 , and ϵ_2 basically represents the wavelength, imaginary and real part of dielectric constant and angular frequency, respectively of the incident light.

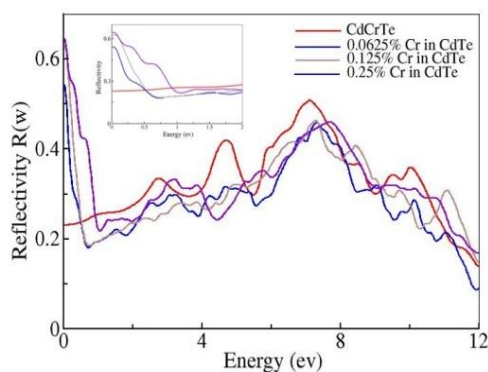


Fig. 4. Reflectivity of pure CdTe and $Cd_{1-x}Cr_xTe$ ($x = 6.25\%$, 12.5% , 25%)

The optical properties of materials can be determined by optical absorption spectrum [29]. The strength of the penetration of light in a material is determined by absorption coefficient. Light is not properly absorbed in those materials which contain low absorption coefficient and thin materials show the transparent behavior for such wavelength. The absorption coefficient basically depends upon the wavelength of light which is being absorbed in the material [30]. Optical properties for pure CdTe compound were calculated and later compared with the Cr doped CdTe compound. In optical properties the cutoff point appeared at 0 eV. The value of absorption coefficient of pure CdTe is minimum at 0.4 eV as illustrated in Fig. 3 (a). By increasing the value of energy, the value of absorption coefficient also increased but after 10 eV the value of absorption coefficient starts to decrease. The highest absorption peaks of pure CdTe, $Cd_{0.9375}Cr_{0.0625}Te$, $Cd_{0.875}Cr_{0.1250}Te$ and $Cd_{0.75}Cr_{0.25}Te$ are appeared at 6.8 eV, 6.7 eV, 7 eV and 6.8 eV and at this energy range the value of absorption coefficients are 140, 127, 133 and 134, respectively. The pure CdTe compound gives the highest peak but after the doping of transition metal at $X = 0.0626$, 0.125% and 0.25% concentration give broader and less pronounced peaks due to inter band transition of transition metal from top most valance band to lowest conduction band. The highest peak of pure CdTe compound appears in the ultra violet region. This means that the material is not transparent in this area. The pure CdTe compound gives the highest peak at 4.5 eV and at this energy the value of optical conductivity was 6803 as shown in Fig. 3 (b).

Similarly, second highest peak of pure CdTe was obtained at 5.8 eV. These both peaks were present in the ultra violet region, but after the doping of transition metal the value of optical conductivity decreases. The refractivity is basically a complex function in which extinction coefficient $k(w)$ represents the imaginary part and refractive index $n(w)$ and represents the real part of the dielectric function. In the Fig.3 (a & b), extinction coefficient and refractive index of Cr doped CdTe compound are plotted versus the energy.

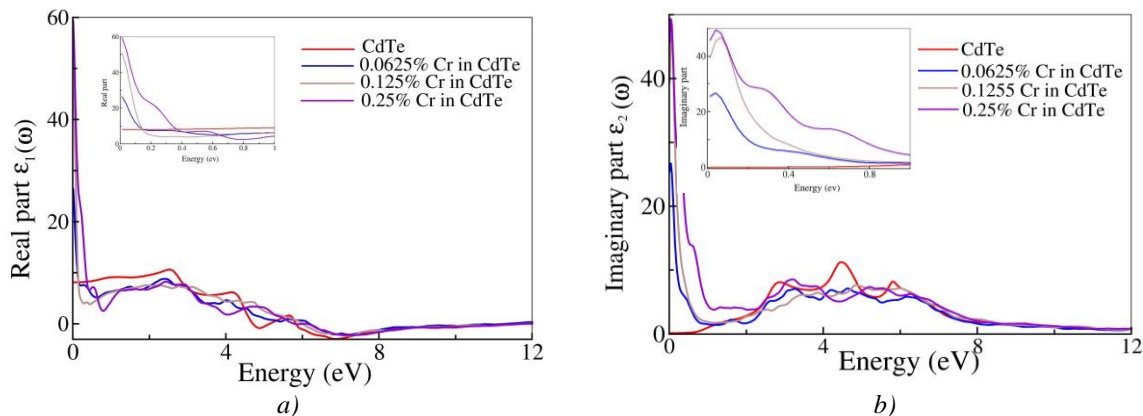


Fig. 5. (a) Real part of dielectric function of pure CdTe and $Cd_{1-x}Cr_xTe$ ($x = 6.25\%$, 12.5% , 25%) (b) imaginary part of dielectric function of pure CdTe and $Cd_{1-x}Cr_xTe$ ($x = 6.25\%$, 12.5% , 25%).

For the study of dissipation and propagation of electromagnetic wave both extinction coefficient and refractive index are studied. The static refractive index is calculated by the static dielectric constant with the following formula.

$$n(0) = \sqrt{\epsilon(0)} \quad (7)$$

The static refractive index $n(0)$ was 2.9 as illustrated in Fig. 3 (a). In the range of 0 to 8 eV, the refractive index $n(w)$ was decreased but after 8 eV the refractive index become constant. Refractive index was 5.6 for $Cd_{0.9375}Cr_{0.0625}Te$, 7.6 for $Cd_{0.875}Cr_{0.1250}Te$ and 8.3 for $Cd_{0.75}Cr_{0.25}Te$, respectively. The intensity of refractive indices decreases with the increase of energy which showed that the refractive index $n(w)$ gradually decreases when the incident photon energy increases. The refractive index of transition metal doped CdTe compound was higher as compared to the refractive index of pure CdTe compound. Fig. 3 (b) shows the minimum and maximum values of extinction coefficient at different energy ranges. First and the highest curve was obtained at 0.1 eV, which means that large amount of absorption occurs at this energy range. Similarly, the small curve was obtained at 1.1 eV which shows that at this energy there was small absorption so the value of extinction coefficient at this energy is minimum. The value of extinction coefficient increases first and then decreases and for higher value of energy it becomes zero. The value of absorption coefficient was higher as compared to refractive index due to this reason it can be used in solar cell industry.

The reflectivity of Cr doped CdTe are illustrated in Fig. 4. The static reflectivity $R(0)$ were 2.3 for pure CdTe and 0.54 for $Cd_{0.9375}Cr_{0.0625}Te$, 0.62 for $Cd_{0.875}Cr_{0.1250}Te$ and 0.64 for $Cd_{0.75}Cr_{0.25}Te$, respectively. For different doping levels, the curves shape and position of reflectivity were quite similar with the curves of extinction coefficient. The highest peak of pure CdTe was obtained at 7 eV and the value of reflectivity was 0.51.

The dielectric function mainly reflects the response of the material to the electric field. The range of energy in imaginary part $\epsilon_2(\omega)$ and real part $\epsilon_1(\omega)$ of dielectric function was kept from 0 to 12 eV. In TM doped compound the real part $\epsilon_1(\omega)$ of dielectric function directs the propagation behavior of the electromagnetic field. Real part $\epsilon_1(\omega)$ showed a negative value which was opposite to the pure structure of CdTe. The negative value of the real part showed that the incident electromagnetic wave are totally reflected, therefore the material represents the metallic nature as shown in Fig. 5(a).

The static real dielectric function $\epsilon_1(\omega)$ for pure CdTe was 8.4 and its lowest peak was appeared at 6.8 eV, the value of real part was -2.9. The cutoff point of imaginary part $\epsilon_2(\omega)$ was 0.3 at 0 eV energy and increases with the energy. At 4.5 eV, it achieves the maximum value 11.5 but after that energy range the value of $\epsilon_2(\omega)$ starts to decrease and become zero. Pure CdTe compound gives the small value of imaginary part but after the doping of transition metal the value

of imaginary part increases. The value of highest peaks were 26, 46 and 49 for $\text{Cd}_{0.9375}\text{Cr}_{0.0625}\text{Te}$, $\text{Cd}_{0.875}\text{Cr}_{0.1250}\text{Te}$ and $\text{Cd}_{0.75}\text{Cr}_{0.25}\text{Te}$, respectively as shown in Fig.5 (b).

3.3. Magnetic properties

The calculated magnetic moment of Cr doped CdTe compound is summarized in Table 1. The total magnetic moments of the compounds were 4.00003, 4.00006 and 4.00017 μ_B for 6.25%, 12.5% and 25% Cr doped CdTe compound, respectively. The partial magnetic moments of Cr were 3.79650, 3.67644 and 3.82310 μ_B for $\text{Cd}_{0.9375}\text{Cr}_{0.0625}\text{Te}$, $\text{Cd}_{0.875}\text{Cr}_{0.1250}\text{Te}$ and $\text{Cd}_{0.75}\text{Cr}_{0.25}\text{Te}$, respectively. It confirms the major contribution of partially filled 3d orbit of Cr. The participation of Te atoms were smaller as compared to Cr and Cd atoms.

Table 1. The interstitials (M_{int}), atom resolved (M_{Cd} , M_{Cr} , M_{Te}) and total magnetic moment of Cr doped CdTe compound.

	M_{int}	M_{Cd}	M_{Cr}	M_{Te}	M_{Tot}
$\text{Cd}_{0.9375}\text{Cr}_{0.0625}\text{Te}$	0.41422	0.01117	3.79650	-0.05891	4.00003
$\text{Cd}_{0.8754}\text{Cr}_{0.1250}\text{Te}$	0.46389	0.02702	3.67644	-0.04776	4.00006
$\text{Cd}_{0.75}\text{Cr}_{0.25}\text{Te}$	0.39256	0.01374	3.82310	-0.06418	4.00017

4. Conclusions

DFT has been used to analyze the electronic, magnetic and optical properties of Cr doped CdTe compound, implemented by WIEN2K code. Transition metal such as Cr doped CdTe compound showed half metallic ferromagnetic behavior with direct band gap nature.

The calculated values of band gap increase from 0.73 to 1.41eV in spin-down states from 6.25% to 25% concentration of Cr and exhibited strong exchange mechanism in all concentrations. The optical results of Cr doped CdTe compound showed the large value of dielectric constants at the low values of energies. Results revealed that Cr doped CdTe (half metallic ferromagnetic) material is suitable for optoelectronic and spintronic applications.

Acknowledgement

1. The author (Shahid M Ramay) would like to acknowledge the Researcher's Supporting Project Number (RSP-2019/71), King Saud University, Riyadh, Saudi Arabia for their partial support in this work .

2. The author (M. Yaseen) thankful to Higher education commission (HEC) of Pakistan for funding through project No: 6410/Punjab/NRPU/R&D/HEC/2016

References

- [1] S. A. Wolf, D. D. Awschalom, R. A. Buhrman, J. M. Daughton, S. Von Molnar, M. L. Roukes, D. M. Treger, Science **294**(5546), 1488 (2001).
- [2] W. E. Pickett, J. S. Moodera, Physics Today **54**(5), 39 (2001).
- [3] R. A. De Groot, F. M. Mueller, P. G. Van Engen, K. H. J. Buschow, Physical Review

Letters **50**(25), 2024 (1983).

- [4] N. A. Noor, S. Ali, S., Shaukat, *Journal of Physics and Chemistry of Solids* **72**(6), 836 (2011).
- [5] K. L. Yao, G. Y. Gao, Z. L. Liu, L. Zhu, Y. L. Li, *Physica B: Condensed Matter* **366**(1-4), 62 (2005).
- [6] I. Galanakis, *Physical Review B* **71**(1), 012413.
- [7] S. P. Lewis, P. B. Allen, T. Sasaki, *Physical Review B* **55**(16), 10253 (2005).
- [8] K. I. Kobayashi, T. H. Kimura, K. Sawada, Y. Terakura, Tokura, *nature* **395**, 677 (1998).
- [9] R. J. Soulen Jr., J. M. Byers, M. S. Osofsky, B. Nadgorny, T. Ambrose, S. F. Cheng, A. Barry, (1998).
- [10] M. Nakao, *Physical Review B* **69**(21), 214429 (2004).
- [11] J. Kobak, T. Smoleński, M. Goryca, M. Papaj, K. Gietka, A. Bogucki, M. Nawrocki, *Nature communications* **5**, 3191 (2014).
- [12] G. Y. Gao, K. L. Yao, E. Şaşıoğlu, L. M. Sandratskii, Z. L. Liu, J. L. Jiang, *Physical Review B* **75**(17), 174442 (2007).
- [13] S. Mackowski, H. E. Jackson, L. M. Smith, J. Kossut, G. Karczewski, W. Heiss, *Applied physics letters* **83**(17), 3575 (2003).
- [14] N. A. Noor, S. Ali, A. Shaukat, *Journal of Physics and Chemistry of Solids* **72**(6), 836 (2011).
- [15] Y. Liu, B. G. Liu, *Journal of magnetism and magnetic materials* **307**(2), 245 (2006).
- [16] J. D. Weidenhamer, F. A. Macias, N. H. Fischer, G. B. Williamson, *Journal of Chemical Ecology* **19**(8), 1799 (1993).
- [17] D. D. Koelling, B. N. Harmon, *Journal of Physics C: Solid State Physics* **10**(16), 3107 (1977).
- [18] P. Hohenberg, W. Kohn, *Physical review* **136**(3B), B864 (1964).
- [19] P. Blaha, K. Schwarz, G. K. Madsen, D. Kvasnicka, J. Luitz, *An augmented plane wave+ local orbitals program for calculating crystal properties*(2001).
- [20] J. P. Perdew, Y. Wang, *Phys Rev B* **45**, 13244 (1992).
- [21] J. P. Perdew, K. Burke, M. Ernzerhof, *Phys. Rev. Lett.* **77**, 3865 (1996).
- [22] M. A. Blanco, E. Francisco, V. Luana, *Computer Physics Communications* **158**(1), 57 (2004).
- [23] D. D. Koelling, B. N. A. Harmon, *Journal of Physics C: Solid State Physics* **10**(16), 3107 (1977).
- [24] P. Hohenberg, W. Kohn, *Physical review* **136**(3B), B864 (1964).
- [25] P. Li, C. W. Zhang, J. Lian, M. J. Ren, P. J. Wang, X. H. Yu, S. Gao, *Optics Communications* **295**, 45 (2013).
- [26] T. Tsafack, E. Piccinini, B. S. Lee, E. Pop, M. Rudan, *Journal of Applied Physics* **110**(6), 063716 (2011).
- [27] G. Murtaza, I. Ahmad, *Physica B: Condensed Matter* **406**(17), 3222 (2011).
- [28] S. Soleimanpour, F. Kanjouri, *Physica B: Condensed Matter* **432**, 16 (2014).
- [29] P. Li, C. W. Zhang, J. Lian, M. J. Ren, P. J. Wang, X. H. Yu, S. Gao, *Optics Communications* **295**, 45 (2013).
- [30] <https://www.pveducation.org/pvcdrom/korean>